Pure and Applied Geophysics

Effects of Surface Geology on Seismic Ground Motion Deduced from Ambient-Noise Measurements in the Town of Avellino, Irpinia Region (Italy)

R. Maresca,[1] L. Nardone,[1] G. Pasquale,[1] F. Pinto,[1] and F. Bianco[2]

Abstract—The effects of surface geology on ground motion provide an important tool in seismic hazard studies. It is well known that the presence of soft sediments can cause amplification of the ground motion at the surface, particularly when there is a sharp impedance contrast at shallow depth. The town of Avellino is located in an area characterised by high seismicity in Italy, about 30 km from the epicentre of the 23 November 1980, Irpinia earthquake ($M = 6.9$). No earthquake recordings are available in the area. The local geology is characterised by strong heterogeneity, with impedance contrasts at depth. We present the results from seismic noise measurements carried out in the urban area of Avellino to evaluate the effects of local geology on the seismic ground motion. We computed the horizontal-to-vertical (H/V) noise spectral ratios at 16 selected sites in this urban area for which drilling data are available within the first 40 m of depth. A Rayleigh wave inversion technique using the peak frequencies of the noise H/V spectral ratios is then presented for estimating Vs models, assuming that the thicknesses of the shallow soil layers are known. The results show a good correspondence between experimental and theoretical peak frequencies, which are interpreted in terms of sediment resonance. For one site, which is characterised by a broad peak in the horizontal-to-vertical spectral-ratio curve, simple one-dimensional modelling is not representative of the resonance effects. Consistent variations in peak amplitudes are seen among the sites. A site classification based on shear-wave velocity characteristics, in terms of $Vs30$, cannot explain these data. The differences observed are better correlated to the impedance contrast between the sediments and basement. A more detailed investigation of the physical parameters of the subsoil structure, together with earthquake data, are desirable for future research, to confirm these data in terms of site response.

Key words: Ambient noise, HVSR, site effects, Avellino.

1. Introduction

There are many site effects that can produce amplification of seismic motion at the surface, including: topography, surface geology and the presence of lateral discontinuities at depth, which can generate two-dimensional (2D) or 3D effects. The simplest situation that produces amplification of seismic motion at the surface arises from the transmission of the seismic waves from a rock medium, usually defined as the bedrock, to the surface sedimentary layers, which are characterised by lower seismic velocities. Under such conditions, the seismic response is evaluated from the spectral ratio between the horizontal *S*-wave component of motion recorded at the surface and at the top of the bedrock (or approximately, at the outcropping bedrock, if it is near enough to the site). This spectral ratio defines the amplification spectrum, i.e. the amplification of the seismic ground motion produced by the surface sediment as a function of the frequency.

The fundamental resonance frequency, which corresponds to the lowest amplification frequency, has been shown to be successfully determined by the horizontal-to-vertical spectral-ratio (HVSR) method, which was applied by NAKAMURA (1989) to microtremors, especially when a sharp velocity contrast is present at depth (RODRIGUEZ and MIDORIKAWA, 2002; SESAME, 2004; DI GIULIO *et al.*, 2008; BONNEFOY-CLAUDET *et al.*, 2009). The *H/V* technique has also been proposed as an alternative tool to classical geophysical exploration for characterising sediment thickness, if the shear-wave velocity profile in the sediment does not change significantly over large areas (IBS-VON SEHT and WOLHENBERG, 1999; PAROLAI *et al.*, 2002). Starting from the reports of NOGOSHI and IGARASHI (1970, 1971), several studies have explained

[1] Dipartimento di Scienze per la Biologia, la Geologia e l'Ambiente, Università degli Studi Del Sannio, Via dei Mulini 59/A, 82100 Benevento, Italy. E-mail: maresca@unisannio.it
[2] Istituto Nazionale di Geofisica e Vulcanologia (INGV), Osservatorio Vesuviano, Naples, Italy.

Ⓑ Birkhäuser

the amplification of the horizontal component of microtremors relative to the vertical component as due to soil-induced modifications of the Rayleigh wave ellipticity (e.g., TOKIMATSU and MIYADERA, 1992; KONNO and OHMACHI, 1998; FÄH et al., 2003; BONNEFOY-CLAUDET et al., 2006). The ellipticity function shows a sharp peak, the amplitude of which depends on the impedance contrast between surface material and deep material. This peak is associated with the vanishing of spectral energy of the vertical component, and with the inversion of the rotation sense of the fundamental Rayleigh wave (SESAME, 2004). MALISCHEWSKY and SCHERBAUM (2004) proposed an analytical formula to interpret H/V measurements in terms of Rayleigh wave propagation. They demonstrated the coincidence between the shear-wave resonance frequency and the peak frequency of the H/V ratio for two-layer models with high impedance contrast. Recent studies have outlined the need to take into account the relative fraction of Rayleigh and Love waves in the horizontal components, to correctly interpret the noise HVSR (ARAI and TOKIMATSU, 2004; KÖHLER et al., 2006; PILZ et al., 2010). BONNEFOY-CLAUDET et al. (2008) proposed a 1D ambient-noise modelling, to determine the reliability of the H/V method. These authors demonstrated that the relative proportion of Love waves in ambient noise controls the amplitude of the H/V peak. However, for 1D horizontally layered structures, they found that the H/V peak frequency always provides a good estimate of the fundamental resonance frequency, whatever the H/V peak origin.

A simple 1D interpretation of the resonance effects may be misleading in cases of 2D or 3D structures: the presence of lateral heterogeneities at depth can generate edge-diffracted waves that can contaminate the noise wave field and make interpretation of the H/V curves difficult (DI GIULIO et al., 2006; MARESCA et al., 2006). The HVSR method also appears not able to evaluate the absolute amplification of the seismic motion, as it gives results that generally do not agree with those coming from methods based on earthquake recordings (LACHET et al., 1996; BARD, 1999; HORIKE et al., 2001; SOURIAU et al., 2007; D23.12, SESAME, 2004; PILZ et al., 2009). The main question regarding the HVSR method concerns the theoretical aspects: whether the

HVSR can be affected by source effects as well as by site effects, and whether body waves or surface waves constitute most of the ambient noise (FÄH et al., 2001; HERAK, 2008). Following KÖHLER et al. (2004), the predominance of Rayleigh waves in the noise wave field can lead to mismatching of the fundamental resonance frequency for low-impedance contrasts.

In the present study, we focused on an examination of the seismic site response in the town of Avellino. This is a small town with a historic midtown and peripheral industries that is located near to the southern Apennines chain, where strong and destructive earthquakes have occurred. The town lies in a structural depression that is filled with deposits that belong to different paleogeographical domains. Because of the lack of earthquake recordings in the urban area of Avellino, we used the HVSR method as applied to microtremors, with the aim of studying the effects on ground motion produced by the local geology. We computed noise HVSRs at 16 measurement sites in the town. Then, on the assumption that the fundamental mode of the Rayleigh waves dominates the microtremor wave field, we applied an inversion procedure on the HVSR data to derive the S-wave velocity models at these sites. We determined whether the noise HVSRs can be interpreted in terms of resonance effects produced by the surface sediments. The HVSR amplitude shows significant variation among the sites. A simple characterisation of the sites in terms of Vs30, as prescribed by the Italian code, does not provide a clear interpretation of these data. The observed variation would be better correlated to differences in the sediment/basement velocity contrast.

2. Seismological and Geological Setting

Avellino is a town located in the Campania Region to the east of Naples, about 30 km from the epicentre of the complex, normal-faulting Irpinia earthquake that caused heavy damage in Avellino (CANDELA and VIGGIANI, 1988). At present, there is background seismic activity, including moderate-sized events (1990, $M = 5.4$; 1991, $M = 5.1$; 1996, $M = 5.1$), that are mainly concentrated around the

three fault segments associated with the Irpinia earthquake (Cocco et al., 1999; Weber et al., 2007).
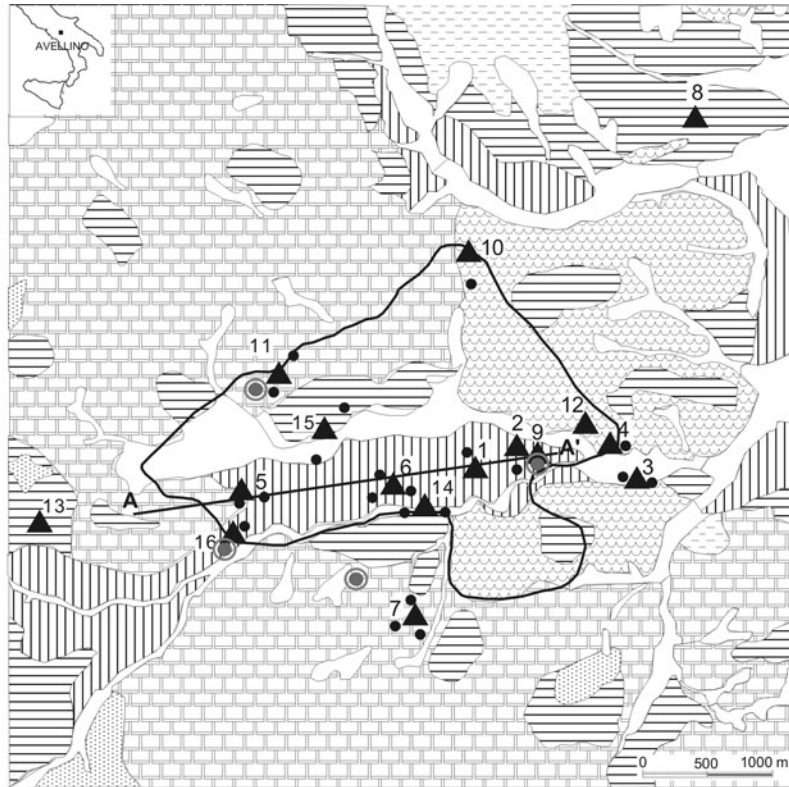
A seismic network of large dynamic range was installed in the Irpinia area recently, to monitor the present seismicity and to provide early-warning analyses (Weber et al., 2007). The seismic hazard in the Irpinia region ranks among the highest in Italy. The peak ground acceleration with a 10% probability of being exceeded in 50 years has been estimated as 0.25 g for this study area (Meletti and Montaldo, 2007). Figure 1 shows a schematic geological map of Avellino, which indicates that the geology is particularly complex due to the presence of deposits that belong to different units (Giulivo and Santo, 1997). Avellino is located at the external border of the calcareous southern Apennines, in a structural depression that is filled with Pliocene deposits, and overlaid by Quaternary formations. The deepest and oldest terrains that are outcropping in Avellino belong to meso-cenozoic basinal successions (Fortore-Groppa d'Anzi Units), which are composed of clay-sandy and marly deposits in the upper part, and by more compact marly-carbonate and siliceous deposits in the lower part. Flysch deposits from the Upper Miocene follow upward through an unconformity boundary; these belong to the Irpinian Supersynthem, as for the Castelvetere formation (Di Nocera et al., 2006). They are composed of coarse-grained sandstone and polygenic conglomerates. These deposits outcrop into the western portion of the urban area, and make up the structure of the surrounding hills. At depth, the roof of this formation is quite regular, and it is at a depth of almost 30 m along the W-E main road alignment in the urban area. Other cenozoic deposits outcrop in the eastern part of Avellino; these consist of grey–blue clay, sand–gravel and pebble cemented deposits, together known as the Tufo–Altavilla group (upper Miocene–lower Pliocene in age). These deposits form a high buried morphological structure below the ancient settlement of Avellino, which has resulted in the raising of the upper tuff formation (see Fig. 1b). The contact between the miocenic deposits is partially hidden by middle Pliocene clastic deposits (mostly conglomerates) that belong to the Ariano-Irpino supersynthem (Di Nocera et al., 2006), as a thickening and coarsening upward succession (of up to 100 m). The conglomerates are made up of polygenic pebble cemented (puddingstone) into a clayey matrix that forms strata or lenses; these have built up the hills to the eastern part of Avellino. The Ignimbrite Campana formation (39,000 y.a.) is the product of a strong eruption that resulted in a wide depression (caldera) that affected the Neapolitan Phlegrean area. The bottom part of this formation consists of cineritic grey tuff crossed by joints. In the upper part, the tuff has yellow facies (zeolite in beds), which are in some places lapideous, and in others weakly cemented. Pyroclastic deposits (the Ottaviano, Pollena and Avellino formations) cover all of these previous geological units. Quaternary alluvial sediments are present in the river valleys as thin lenses, and in some places ancient alluvial deposits are buried below the Ignimbrite Campana formation. Figure 1b shows a schematic geological section across the town, the location of which is shown in Fig. 1a. Figure 1a also shows the locations of the sites where the noise measurements were carried out, and the locations of the drilling holes and seismic down-holes. The topography in the urban area is almost regular, gently rising from the southern hill zone to the North. The maximum height difference in the area investigated is of about 70 m, between sites 7 and 8. The drilling data and seismic down-holes were produced by the local council (Comune di Avellino, Piano Regolatore Generale, 2003), with a view to urban planning. Cores extracted from drillings give the litho-stratigraphic features to a maximum depth of 40 m.

3. Measurements

Noise measurements were executed during three experiments carried out in 2005 (7 July) and in 2008 (10 and 25 January; 22 December). We used a digital Lennartz/MarsLite recording station, coupled to a LE/3D/1 s sensor. The sample rate was 125 cps. We recorded 30 min of noise at each site. An example of the recording at two sites is given in Fig. 2. Notably, site 1 is located in downtown Avellino (Piazza Libertà); the noise measurements were carried out in the daytime, when there was a lot of vehicle traffic, as shown by the higher amplitude of the ground velocity measured at this site.
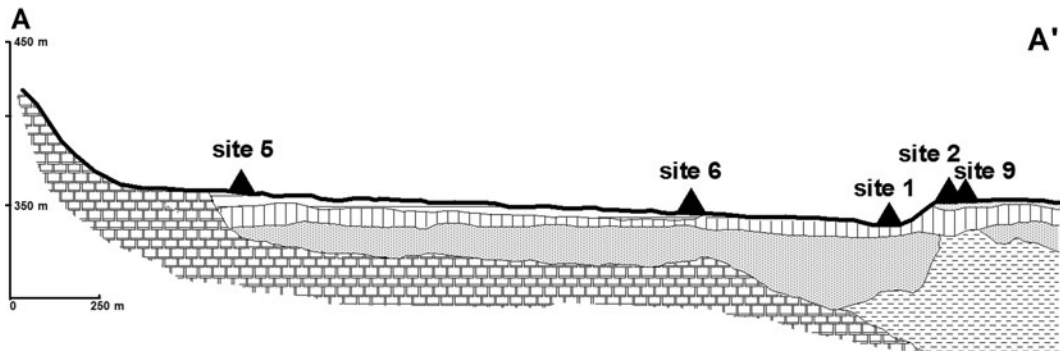
A

debris (Holocene)   conglomerate (Pleistocene - Pliocene)

alluvium (Holocene)   clay and sand-gravel (Miocene)

pyroclastite (Hol.)   sandstone (Early Mioc. - Late Creta.)

tuff (Early Pleist.)   silty sand (Early Pleist.)

▲13 measurement sites   • drilling holes   ◎ down-holes

A⟋A' trace of geological profile   ⬭ historical centre of Avellino

B

◄

Figure 1
a Schematic geological map of Avellino, with the location of the noise measurement sites, drill holes and down-holes, and the trace of the geological profile. **b** Geological profile across the downtown area. Legend as for (**a**)

For each of the measurement sites, we propose a simplified stratigraphical section shown in Fig. 3, which is extrapolated from the drilling lithological data; the drilling locations are shown in Fig. 1. Site 9 is located at the top of a manmade terrace, in a construction area. The top layer is formed by filling materials, the thickness of which was evaluated in the field (6 m). For this site, and for others, the upper thin layer of recent deposits depicted in the section is not mapped in Fig. 1a. This is due to the small thickness of the cover materials. No drilling data are available for sites 8 and 13, and their stratigraphies were schematised on the basis of field observations. These sites are located within two construction areas and the measurements were carried out on an excavation floor, where the basement outcrops (site 8_{down} and 13). At site 8, the measurements were also taken at the top of

outcropping sediments (8_{up}), at a horizontal distance of about 3 m from the bottom rock-measurement point. Site 7 has similar characteristics to site 8. Similarly, we defined two measurement points: at the top of outcropping sediments (7_{up}) and vertically below the 7_{up} position, at the basis of an excavation where the basement outcrops (7_{down}). The sediment thicknesses at measurement points 7_{up} and 8_{up} were evaluated on the excavation walls, as 7 and 11 m, respectively.

The description of the litho-codes is given in Table 1, together with the ages, the *Vs* and the density ranges of values, and the Poisson coefficient. To assign the shear-wave velocity classes of values to each lithotype, we considered the classes of wave-velocity values estimated from seismic refraction and down-hole measurements provided by the municipality of Avellino (Piano Regolatore Generale, 2003) for the outcropping deposits (Table 2). For lithotypes that were not examined by seismic surveys, we took into account the site classifications proposed by the International Conference of Building Officials (NEHRP-UBC, 1997) and by the Italian government
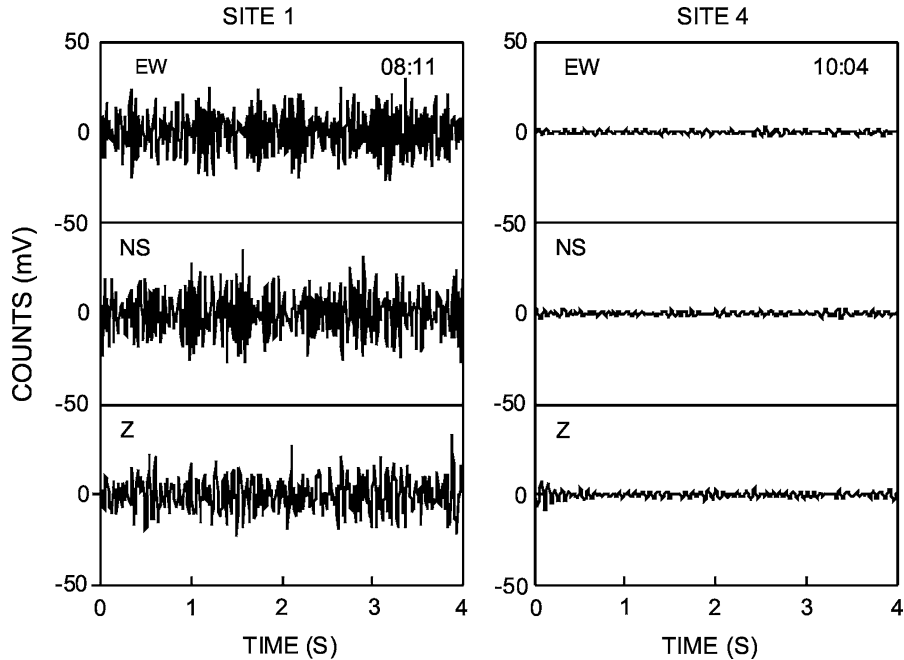

Figure 2
Three components of the ground velocity over a 5-min window of seismic noise recorded at sites 1 and 4 on 6 July 2005. Site code and start time of the record are shown at the upper right of each plot. The traces are plotted using the same scale. Note the higher amplitude recorded at site 1
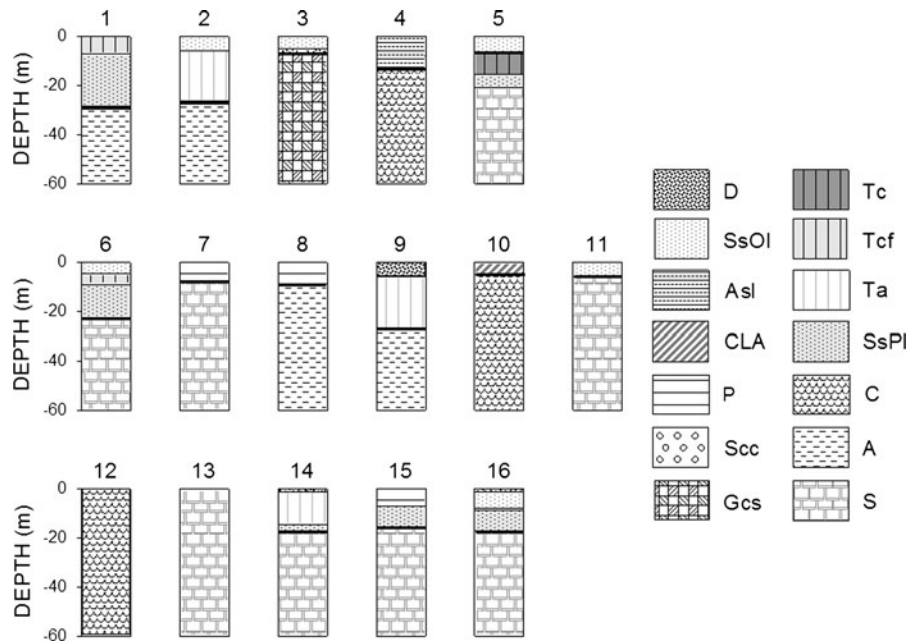
Figure 3
Lithological sections of the sites investigated, as indicated. The lithotype codes are defined in Table 1. The *thick line* marks the top of the lithotype, which is considered as the basement when computing of the amplification functions

(NTC, Norme Tecniche per le Costruzioni [NTC]; D.M. 14/01/2008) (Table 3). The Poisson ratio values were estimated on the basis of the seismic velocity measurements reported in Table 3. The density classes were taken from the literature (CLARK, 1966). Different velocities were assigned to the same lithotypes of different ages, to allow for the differences in elastic properties that correlate with the ages of the rock formations. Moreover, for the same geological formation, as with the Ignimbrite Campana tuff, we can distinguish different lithotypes, with regard to the degree of hardness, and hence, to the elastic properties.

To compute the spectral ratio between the horizontal and the vertical components of the ground velocity for each site, we used the JSESAME software (European Commission—Project No. EVG1-CT-2000-00026 SESAME. WP03—*H/V* Technique). This software is based on automatic window selection (anti-trigger algorithm) to keep the most stationary parts of the noise. The parameters used in the anti-trigger modulus were chosen according to the SES-AME criteria (SESAME, 2004) and are reported in
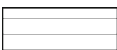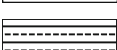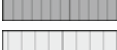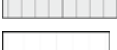
Table 4. A different number of time-windows (t-win) that were derived from the anti-trigger modulus were selected at the sites, as shown in Table 5. Then the following procedure was performed: (a) 5% cosine tapering; (b) fast Fourier transform; (c) KONNO and OHMACHI (1998) smoothing: $b = 20$; (d) Merging of the two horizontal components with the quadratic mean; (e) HVSRs for each time window; (f) Average HVSRs and error estimates.
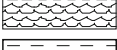
The b value is a coefficient for the band width in the smoothing function. It has been shown that this parameter influences not only the *H/V* peak amplitude, but also the peak frequency (KONNO and OHMACHI, 1998). To choose an appropriate value for this parameter, we performed a test, computing the HVSRs with $b = 10$, 20 and 40. We observed only small differences in the peak values and a slight decrease in the peak frequency for the lowest b value. We therefore applied a smoothing function with $b = 20$.

In Fig. 4, the mean noise HVSRs are shown (thick lines), together with the $\pm 1\sigma$ curves (thin lines) for each sediment site. Following the criterion of

Table 1

Description of the lithotypes that characterise the first 60 m of stratigraphy at the sites

Code		Lithology	Age	Vs (m/s)	σ	ρ (g/cm³)
D		Debris	Holocene	100–180	0.40	1.2–1.4
SsOl		Silty sand	Holocene	100–300	0.40	1.2–1.4
CLA		Heterometric clasts in silty clay matrix	Holocene	180–300	0.40	1.2–1.4
P		Clayey pyroclastite	Holocene	200–380	0.40	1.2–1.4
Asl		Sand and silty clay with clasts	Holocene	180–360	0.40	1.3–1.5
Scc		Sand with calcareous clasts	Holocene-Early Pleistocene	360–550	0.40	1.4–1.8
Gcs		Calcareous gravel with sandy matrix	Holocene- Early Pleistocene	360–700	0.36	1.4–1.8
Tc		Compact tuff	Early Pleistocene	700–1,000	0.35	1.4–1.8
Tcf		Compact fractured tuff	Early Pleistocene	500–700	0.35	1.3–1.7
Ta		Disaggregated tuff	Early Pleistocene	400–500	0.35	1.3–1.7
SsPl		Silty sand	Early Pleistocene	200–400	0.40	1.2–1.5
C		Conglomerate	Pleistocene-Pliocene	700–1,000	0.36	1.6–2.0
A		Clay and sand-gravel	Miocene	700–1,000	0.40	1.6–2.0
S		Sandstone	Early Miocene-Late Cretaceous	800–1,200	0.35	1.6–2.0

Vs shear wave velocity, *σ* Poisson ratio, *ρ* density

classification proposed by BONNEFOY-CLAUDET *et al.* (2009), the spectra are separated into three groups, according to their shapes: with a clear maximum peak (>5) (Fig. 4, upper panel); flat HVSR curves with low amplitude (Fig. 4, central panel); and with a broad peak, that in some cases (site 15) appears as a plateau extending at low frequency (Fig. 4, bottom panel). For some sites, a minor peak at a frequency of about 1–2 Hz is seen. The discontinuity within the deepest meso-cenozoic deposits (Fortore-Groppa d'Anzi Units), between the upper clayey/marly member and the lower most compact calcareous/siliceous member, might represent the deep horizon below the engineering bedrock that caused this peak. Other geophysical data at a different scale would be necessary to model this characteristic.

In Fig. 5, we have plotted the mean noise HVSRs computed for all of the sites characterised by the basement outcropping (rock sites). The ratio remains fairly low for all of these sites, as expected for rock sites. In Fig. 6, we show the results obtained at sites 7 and 8, which are characterised by two measurement points (*up*: cover sediments; *down*: basement). The upper panels of Fig. 6 show the mean HVSR curves computed at the surface and at the basement. The HVSR curves computed at the surface reach values >2 in the frequency band 4–12 Hz. This effect is better evident for site 8: the HVSR curve computed at this site is characterised by a prominent wide peak, followed by a sharp drop, which corresponds to a minimum zone in the vertical spectrum. The sharp drop which follows the peak can help in the

Table 2

Classes of values of seismic-wave velocities for the main lithotypes that outcrop in Avellino, from seismic refraction and down-hole measurements (Comune di Avellino, Piano Regolatore Generale, 2003)

Lithology	V_P (m/s)	V_S (m/s)
Alluvial gravel	660–1,000	250–400
Pyroclastite	200–400	90–140
Clayey pyroclastite	600–900	200–380
Tuff	1,100–1,700	450–1,000
Compact clay	2,000–2,500	900–1,000
Conglomerate	1,700–1,900	700–1,000

Table 3

Site categories, as defined by the Italian Government (NTC, Norme Tecniche per le Costruzioni. D.M. 14/01/2008, G. U. no. 29, 04/02/ 2008) and by the International Conference of Building Officials (NEHRP-UBC, 1997)

Description	NTC		NEHRP-UBC	
	Soil type	Vs30 (m/s)	Soil type	Vs30 (m/s)
Rock	A	>800	A–B	>760
Very dense soil	B	360–800	C	360–760
Middle dense, stiff soil	C	180–360	D	180–360
Poorly dense soil	D	<180	–	–
Soft soil	E	<180	E	<180

These classifications use the average shear-wave velocity to 30 m (*Vs30*) as an indicator of site response

Table 4

Parameters used in the anti-trigger modulus for window selection to compute the H/V spectra (JSESAME software)

Parameter	Value
Sta length	1 s
Lta length	25 s
Minimum sta/lta	0.5
Maximum sta/lta	2
Window length	16 s

Table 5

Number of time windows (t-win) of noise signal recorded at the sites that were selected to compute the HVSRs

Site	No. t-win.	Site	No. t-win.
1	64	8 down	18
2	57	9	74
3	35	10	62
4	31	11	26
5	13	12	55
6	42	13	19
7 up	8	14	21
7 down	61	15	28
8 up	16	16	16

4. Data Analysis

With the hypothesis that noise HVSR is basically related to the ellipticity of the fundamental mode of Rayleigh waves that composes the noise, we attempted an inversion of the HVSR peak frequencies, with the purpose of deriving the *S*-wave velocity profiles at these sites. The presence of Love waves in the noise wave field can also affect the HVSR signature. Nevertheless, we believe that the Rayleigh waves hypothesis can be valid, as the inversion is applied only to the HVSR peak frequencies, which fit the Rayleigh waves ellipticity well, at least for strong impedance contrasts.

We used the computer programme DINVER, a tool for solving inversion problems with the Neighbourhood Algorithm (WATHELET et al., 2008). Unlike classical inversion methods, the neighbourhood algorithm allows searches to find models of acceptable data fits by investigating the whole parameter space. The programme computes the Rayleigh wave ellipticity function in a layered half-space. The site model is characterised by a sequence of *n* layers that

identification of the fundamental resonance frequency (KONNO and OHMACHI, 1998). The secondary peak, which is observed in the HVSR curve measured at site 8$_{up}$ in the frequency band 1–2 Hz, is also present as the maximum peak in the 8$_{down}$ HVSR curve. As discussed above, this peak might be associated with a deeper discontinuity within the basement formation. The spectra computed at the *down* measurement points have lower amplitudes, as compared to the surface measurements. The 7$_{down}$ spectra show moderate peaks in the frequency band 4–7 Hz. These peaks are present with different amplitudes on all of the spectral components, and are maybe not associated with the sediment/bedrock structure (CASTELLARO and MULARGIA, 2010).

overlay the basement, each of which is defined by the parameters of thickness, *P*-wave velocity, *S*-wave velocity, and density (*h, Vp, Vs, ρ*).

To define the initial site models, we referred to the stratigraphic sections shown in Fig. 3, and to the classes of parameters reported in Table 1 for each lithotype. Sites 14 and 16 have a very thin layer within the stratigraphy (Fig. 3). We proposed simplified initial models for these sites, which included the thin layer within the adjacent layer with the most similar properties. This is because the inversion of the data might not be reliable due to a lack of resolution of the surface waves for these thin layers. Sites 12 and 13 are excluded from the computing, as they are considered as rock sites. For most of the sites, we considered the seismic basement as both the meso-cenozoic formations and the miocenic flysch formation, which are the deepest and oldest deposits that outcrop in Avellino, as described in Sect. 2 above. In other cases (sites 3, 4 and 10), the younger, but compact, conglomerate or gravel formations are used as the seismic basement. Site 5 has a succession of holocenic silty sand (7 m thick), tuff (9 m thick), and pleistocenic silty sand (5 m thick) that overlay the

clayey meso-cenozoic basement. As described by the available stratigraphic data, the tuff layer is well compacted at this site (lithotype *Tc*, in Table 1), so we assigned a shear-wave velocity of 700–1,000 m/s for this, higher than the values assigned to this lithotype for the other sites (*Tcf, Ta*, in Table 1). A first comparison between the theoretical and experimental functions at this site allowed us to establish that the sediment–tuff impedance contrast is the most significant for generating resonance effects. Therefore, in the inversion procedure, we retained the tuff formation as the seismic basement for site 5. The inversion was performed on the peak frequencies of the HVSR curves. This parameter controls both the velocity and the thickness of the layers. We performed a first block of 50 iterations (2,550 models) of the neighbourhood algorithm, allowing *Vs* to vary within the range of values defined in Table 1 (Fig. 7, dashed lines in left-hand plots), and fixing the other parameters. The layer thickness was known from independent measurements. The knowledge of this parameter allows us to overcome the trade-off between velocity and layer thickness (SCHERBAUM *et al.*, 2003). The density and Poisson ratio were fixed as the average values of
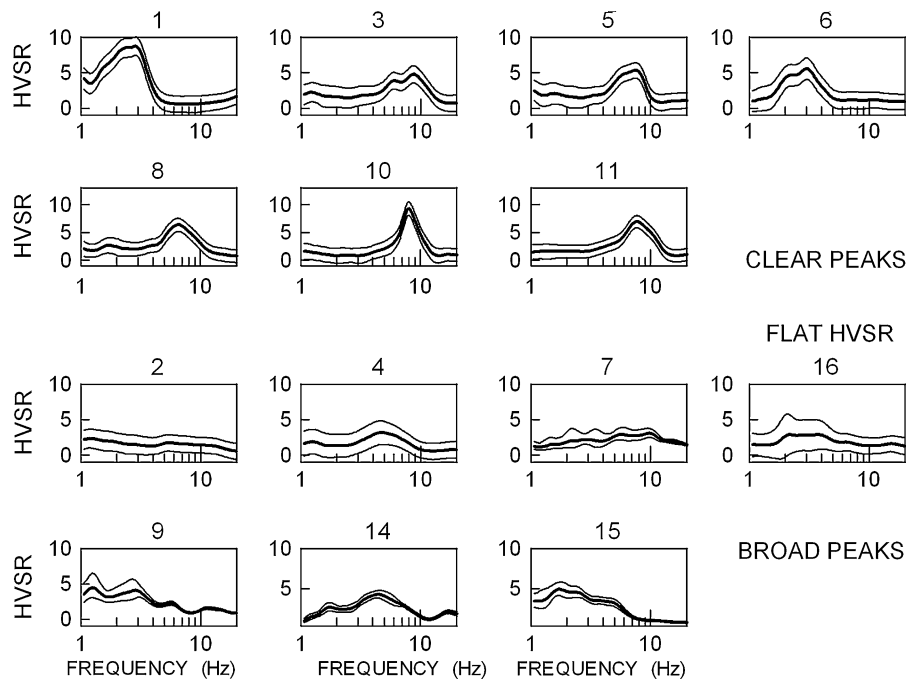

Figure 4
Mean noise HVSRs (*thick lines*) and ±1σ curves (*thin lines*) at all of the sediment sites
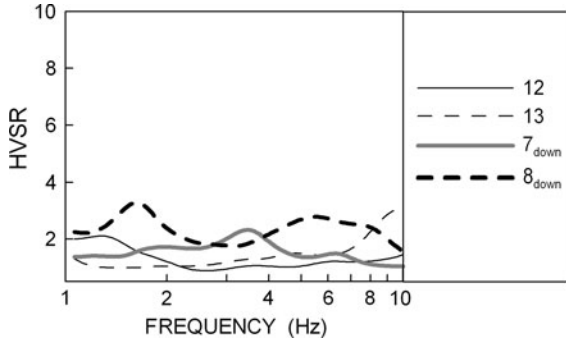
Figure 5
Mean HVSRs computed at the outcropping basement for sites 7, 8, 12 and 13
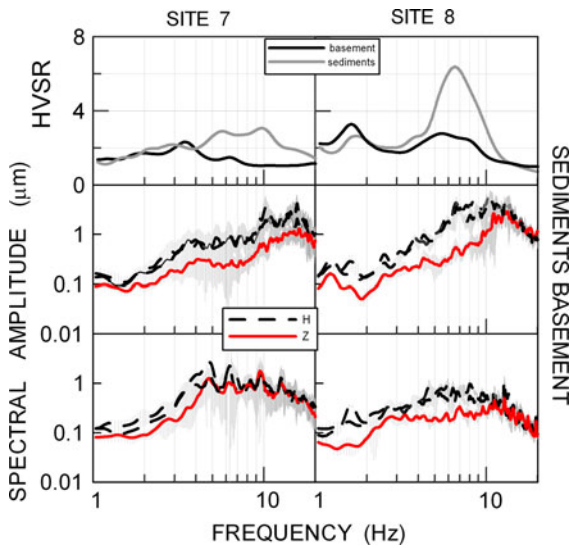

Figure 6
Upper panels Sites 7 and 8 (as indicated), as comparisons of HVSRs computed at the surface and the basement. Central panels: Mean spectral amplitudes computed at the surface sediments for the horizontal and vertical components. The spectral amplitudes were computed following the procedure described in Table 6. *Vertical bars*, standard deviations. *Lower panels* Mean spectral amplitudes computed at the basement for the horizontal and vertical components. The spectral amplitudes in *central* and *lower panels* were corrected for instrument response

the ranges reported in Table 1 for each layer. Finally, using the best-fit final models as initial models, we performed a second block of 50 iterations, leaving Vs to vary within 20% of the best value obtained after the first 50 iterations.

The computed curves are shown in Fig. 7, where they are compared to the noise HVSR curves; the Vs

models are depicted to the left of each plot. The red curve corresponds to the model that produces the minimum misfit function. The misfit function is defined as:

$$\text{misfit} = \sqrt{\sum_{i=1}^{n} \frac{(f_P)_{\text{observed}} - (f_P)_{\text{calculated}}}{(df_P)_{\text{observed}}}} \quad (1)$$

where f_P if the frequency of the peak, and (df_P) is the standard deviation of the experimental frequency peak. The S-wave velocity of layers up to the basement are well constrained; the largest uncertainties are associated with the half-space parameters.

We can compare the results obtained at sites 11 and 16 with the Vs down-hole measurements obtained in proximity to the sites (Table 7). The comparison for site 11 is good (differences within 13%); the Vs values estimated from the inversion at site 16 differ by 20–50% with respect to the down-hole data, with the biggest differences in the surface layers. The best-fit model obtained at site 16 shows a high misfit value, due to the high dispersion associated with the data, and this might be the reason for the discrepancy in the Vs values.

Sites 2 and 9, which are located very close to each other in the historical centre of Avellino, have a similar geological structure. Using the site models defined from the drilling data down to 40 m in depth, we obtained unconstrained results. We observed that some noise HVSR spectra show a moderate peak at 1–2 Hz, which for sites 2 and 9 is the maximum peak. With reference to the geology of the area, we assume the presence of a deep interface to explain this peak. Evidently, this deep interface produces the main effect for these two sites, and further data at different scales would be necessary to model them.

It has been experimentally shown that the HVSR method can predict the resonance frequency of sediments, although it cannot be used to estimate the absolute values of the seismic amplification (see Sect. 1). Here, there are significant differences in the HVSR amplitudes measured at the sediment sites, which vary from 2 to 9 (Fig. 8). To determine whether the differences observed are significant in terms of site response, a comparison with earthquake data would be advantageous. However, due to the lack of earthquake recordings in the urban area of Avellino,
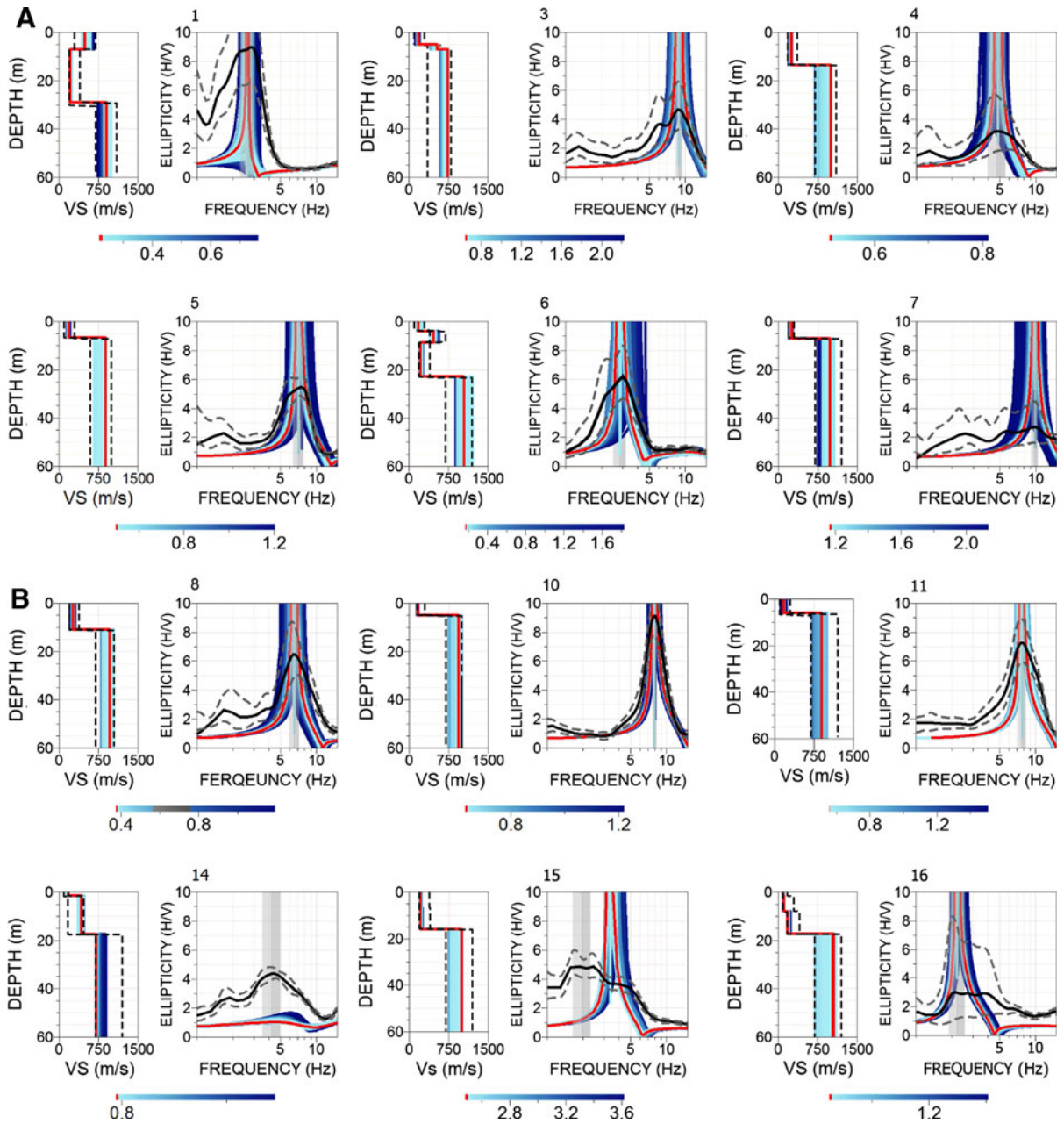
Figure 7

The HVSR inversion. *Left* Vs models. *Dashed lines*, the starting model space. *Right* Ellipticity function and observed HVSR (*solid black line*) ±1 σ (*dashed black lines*). *Red lines*, the minimum misfit. *Blue scale colour*, the misfit associated with the model space for the final run (2,550 models)

we can only propose a qualitative analysis. The recent mapping of the site conditions has grouped the geologic units with similar shear-wave velocity characteristics, in terms of *Vs30* (BORCHERDT *et al.*, 1991; WILLS *et al.*, 2000). As the HVSR cannot

provide absolute amplification, this simple approach is here limited to an analysis of variations among the sites.

In Fig. 9, we have plotted the HVSR peak *versus* the *Vs30* estimated from the *Vs* inverted profiles.

Table 6

Procedure steps to obtain the velocity spectra

Average removing
Windowing by ten 2,048-point-long windows
Fast Fourier transform on each window
Computing average spectrum
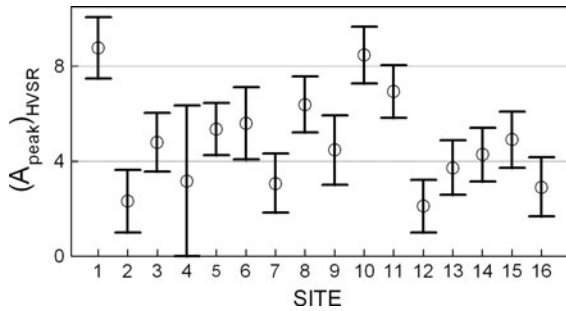Triangle-window/moving-average smoothing

Figure 8
Peak amplitude in the HVSRs for all of the sediment sites. *Error bars* indicate $\pm 1\,\sigma$ of the values

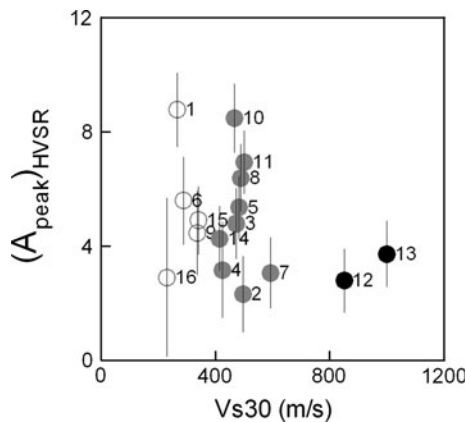Figure 9
Peak amplitude of the noise HVSRs as a function of the *Vs30*. Different symbols are associated with different soil classes, as ascribed by the National code (NTC, 2008), to which the sites under investigation belong. *Black circles*, class A; *grey circles*, class B; *open grey circles*, class C

Different symbols are associated with different soil classes, as ascribed by the National code (NTC, 2008), to which the sites under investigation belong (see Table 8). We see good correspondence for the class A sites (Fig. 9, black circles), which are characterised by a *Vs30* greater than 800 m/s and the lowest amplitude in the HVSRs. However, no

Table 7

Vs down-hole profiles (Comune di Avellino, Piano Regolatore Generale, 2003)

Site	Thickness (m)	Vs (m/s)
Site 11	6	160
	24	770
Site 16	6	180
	8	310
	6	700
	10	860

Table 8

Classification of the noise measurement sites with respect to the Italian Official code (NTC, 2008)

Site	NTC category
12, 13	A
3, 4, 5, 7, 8, 10, 11, 14, 15	B
1, 2, 6, 9, 16	C

correlation between *Vs30* and HVSR peak amplitude is seen for the sites of class B ($360 < Vs30 < 800$ m/s) (Fig. 9, grey circles) and class C ($180 < Vs30 < 360$ m/s) (Fig. 9, open grey circles). As also shown by other authors (MUCCIARELLI and GALLIPOLI, 2006; CASTELLARO and MULARGIA 2008; LUZI *et al.*, 2011), *Vs30* is often an inappropriate parameter for describing site effects. Reasonably, *Vs30* cannot correlate with the HVSR peak when there is a sharp velocity contrast within the first 30 m of depth.

As discussed in the previous paragraph, we computed the shear-wave profiles on the assumption that the HVSR can be modelled with the ellipticity of the fundamental mode of Rayleigh waves. The shape of the noise HVSRs, as well as the shape of the *H/V* ellipticity ratios of the Rayleigh waves, are influenced by the velocity structure. A strong velocity contrast produces a clear peak in the experimental curve and an infinite peak in the theoretical curve, very close to the fundamental resonance frequency. Then we would determine whether the amplitude of the peak in the HVSR curves can be correlated with the velocity contrast between the sediments and the basement $((Vs)_{basement}/(Vs)_{sediments})$.

We computed the velocity contrast with reference to the best-fit shear-wave velocity models. The
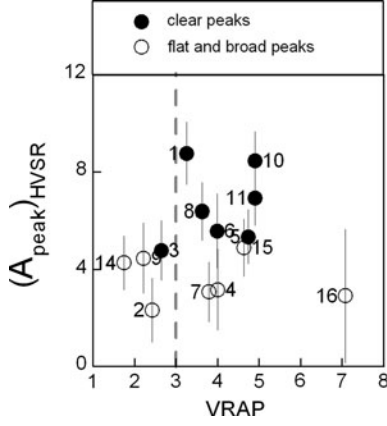
Figure 10
Peak amplitude of the noise HVSRs as a function of the velocity ratio between the basement and the sediments. *Error bars* indicate $+1\sigma$ of the values

average shear-wave velocity in the sediments was computed according to the formula:

$$\langle V_S \rangle = \sum_n h_i \Big/ \sum_n \left(h_i / (V_S)_i \right) \qquad (2)$$

where h_i is the layer thickness and n is the number of sediments layers. For sites 2 and 9, we used the average *Vs* values over the ranges reported in Table 1. In Fig. 10, we have plotted the HVSR peak amplitude *versus* the velocity contrast between the sediments and the basement. Here, the sites that have clear peaks in the HVSR curves (Fig. 10, black circles) have high velocity contrast (>3), except for site 3. Nevertheless, there are also some flat or broad peaks (sites 4, 7 and 16) that appear for high velocity contrasts. Site 16 is characterised by large dispersion of the data, and this could explain the anomalous result. We cannot justify the results obtained for sites 4 and 7, which were modelled with an impedance contrast that varies from 3 to 4, and which show low HVSR amplitudes. Following BONNEFOY-CLAUDET *et al*. (2009), flat and low HVSR curves should correspond to low velocity contrasts. Potentially, the uncertainty associated to the half-space parameters biases these results. Further in situ measurements, such as down-hole seismic logging, would better constrain these data.

As suggested by KÖHLER *et al*. (2004), the velocity contrast can also influence the peak frequencies when the noise wave field is mostly composed of Rayleigh
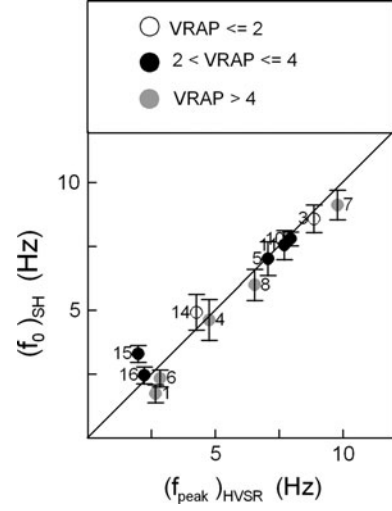

Figure 11
Fundamental resonance frequencies for the shear waves as a function of the peak frequencies in the experimental HVSRs. Line, the $y = x$ curve. The *error bars* indicate $\pm 1\ \sigma$ of the values

waves. Indeed, the peak frequency in the theoretical ellipticity ratio can not be in agreement with the fundamental resonance frequency for low velocity contrast. To determine the goodness of the HVSR measurements to predict the resonance of the sediment, the inverted *Vs*-profiles were used to model the *SH*-transfer function for the sites, following the approach described by KRAMER (1996). The damping factor was considered constant, and was set to 0.05. The density was fixed to the average value in the ranges reported in Table 1 for each layer. In Fig. 11, we have plotted the peak frequencies in the HVSR curves *versus* the fundamental frequencies of the *SH*-transfer functions. The sites are classified according to the velocity contrast. There is relatively good correlation between the frequencies, whatever value of the velocity contrast is at depth. Except for site 15, the differences between the HVSR peak frequencies and the *S*-wave resonance frequencies are included within the measurement uncertainties. The results shown in Fig. 11 suggest that noise HVSRs are a valid tool for the estimation of the resonance frequencies of surface sediments, within the uncertainty limits. The HVSR measured at site 15 shows a broad amplitude peak, and identification of the peak frequency might be inaccurate. Potentially, a simple 1D structure cannot be representative for this site.

5. Conclusions

This study deals with the assessment of site effects in the city of Avellino, Italy. For this purpose, we performed ambient-noise measurements at 16 sites and processed these according to the HVSR technique. On the assumption that the fundamental mode of the Rayleigh waves is predominant in the noise wave field, we applied an inversion procedure to the HVSR peak frequencies, with the aim of obtaining the *Vs* profiles. As has been proposed by many authors (Fäh *et al*., 2001; Scherbaum *et al*., 2003; Wathelet *et al*., 2008), this assumption is based on the frequency dependence of the ellipticity of the Rayleigh waves as a response to the site structure. Love waves can also contribute to the horizontal motion generated by the noise wave field, mostly influencing the amplitude of the HVSR peak. Based on the inverted shear-wave velocity models and, for unresolved cases, also on data coming from drilling and seismic prospecting, we computed the basement/sediment velocity contrasts, which were correlated with the peak frequencies and the peak amplitudes in the HVSRs.

Our main conclusions here can be summarised as:

1. The geology of Avellino is complex because of the presence of different outcropping lithotypes; for each site, we produced a stratigraphic profile on the basis of drilling data. At some of the sites, the results were different, even if they have the same kind of soil. This indicates that the velocity can vary significantly for the same kind of soil, according to the degree of hardness and to the age of the deposits. This peculiarity should be carefully considered when planning accurate microzonation surveys.

2. The effects of impedance contrast on the HVSR peak and the relationship with the *S*-wave fundamental frequency has been studied by many (Konno and Ohmachi, 1998; Malischewsky and Scherbaum, 2004; Köhler *et al*., 2004), which show that the hypothesis of a noise wave field mostly composed of Rayleigh waves can be misleading for low velocity contrasts. We generally observe that the noise HVSR peak frequencies are in agreement, within the uncertainty limits, with the direct *S*-wave resonance frequencies, also for the lowest velocity contrasts. These results, which can be considered preliminary in Avellino as they are from limited data samples, suggest that noise HVSR measurements can be effective in the evaluation of the resonance frequencies, whatever the value of the impedance contrast at depth, provided that a 1D structure is present. Site 15 shows the highest differences between the computed and experimental frequencies: the HVSR measured at this site has a broad amplitude peak, which was probably generated by a more complicated subsurface structure, and the identification of the peak frequency is ambiguous.

3. It has been shown by a lot of experimental evidence that the *H/V* method cannot predict the amplification of seismic ground motion at the surface. The *H/V* spectral amplitudes are significantly influenced by the smoothing function (Konno and Ohmachi, 1998), and a comparison with theoretical amplification functions cannot be effective: the peak values in the computed *H/V* ratio are strongly affected by the sediment/basement impedance contrast, with infinite peaks in the case of strong contrast at depth. Also, the peak amplification in the SH transfer function depends on the damping in the sediments, which is often unknown. As the HVSR cannot provide absolute amplification, we can only propose a qualitative interpretation of these results, which is limited to the analysis of the variations among the sites. HVSR amplitude peaks measured in Avellino show differences from site to site, which cannot be justified by a simple characterisation of the sites in terms of the *Vs30*, as prescribed by law. Based on these observations, we suggest that the knowledge of the *Vs30* appears to be insufficient to characterise the sites, and a velocity profile down to the bedrock should be taken into account. HVSR amplitude peaks should be better correlated to the velocity contrast at depth.

This study is the first to describe the effects of surface geology on seismic ground motion in Avellino using ambient noise measurements. The analysis is based on limited data and on a simplified hypothesis concerning the nature of the noise wave-field.

Microtremor array analysis combined with a denser grid of HVSR data would be suitable to provide more accurate estimates of the subsoil velocity structures and to define the spatial distributions of the resonance frequencies in the whole urban area. An inversion considering higher modes and Love waves, which produce significant effect on the peak amplitude, might also be proposed for future studies, in better constraining uncertain data, especially regarding the half-space parameters. If earthquake data are available in the future, these would be fundamental to verify the noise data and to provide the absolute amplification of the ground motion.

References

ARAI, H., and TOKIMATSU, K. (2004), *S-wave velocity profiling by inversion of microtremor H/V spectrum*, Bull. Seism. Soc. Am., *94*, 53–63.

BARD, P.Y. (1999), Microtremor measurements: a tool for site effect estimation?, Proc of the 2nd Int. Symp. on Effects of Surface Geology on Seismic Motion, Yokohama, Japan, 1-3 December, *3*, 1251–1282.

BONNEFOY-CLAUDET, S., CORNOU, C., BARD, P.Y., and COTTON, F. (2006), H/V ratio: a tool for site effects evaluation. Results from 1-D noise simulations, Geophys. J. Int., **167**, 827-837.

BONNEFOY-CLAUDET, S., KÖHLER, A., CORNOU, C., WATHELET, M., and BARD, P.Y. (2008), *Effects of Love waves on microtremor H/V ratio*, Bull. Seism. Soc. Am., *98*, 288–300.

BONNEFOY-CLAUDET, S., BAIZE, S., BONILLA, L.F., BERGE-THIERRY, C., PASTEN, C., CAMPOS, J., VOLANT, P., and VERUGO, R. (2009), Site effect evaluation in the basin of Santiago de Chile using ambient noise measurements, Geophys. J. Int., **176**, 925-937.

BORCHERDT, R.D., WENTWORTH, C.M., JANSSEN, A., FUMAL, T., and GIBBS, J. (1991), Methodology for predictive GIS mapping of special study zone for strong ground motion in the San Francisco Bay region, CA., In Proc. Fourth Int. Cont. on Seismic Zonation, Earthquake Engineering Research Institute, Oakland, California, 545–552.

CANDELA, M., and VIGGIANI, C. (1988), The effects of the Irpinia earthquake in the ancient centre of Avellino, Italy, Proc. Inter. Symp. IAEG, Athens, Greece, 1988.

CASTELLARO, S., and MULARGIA, F. and ROSSI P.M. (2008), *VS30: proxy for seismic amplification*?, Seism. Res. Lett. **79**, 540–542.

CASTELLARO, S., and MULARGIA, F. (2010), *How far from a building does the ground-motion free-field start?*, Bull. Seism. Soc. Am., *100*, 2080–2094.

CLARK, S.P. (1966), *Handbook of physical constants*, Geol. Soc. Am., Mem., *97*.

COCCO, M, CHIARABBA, C., DI BONA, M., SELVAGGI, G., MARGHERITI, L., FREPOLI, A., LUCENTE, F.P., BASILI, A., JONGMANS, D., and CAMPILLO, M. (1999), *The April 1996 Irpinia seismic sequence: evidence for fault interaction*, Journ. Seismol., *3*, 105–117.

DI GIULIO, G., CORNOU, C., OHRNBERGER, M., WATHELET, M., and ROVELLI, A. (2006), *Deriving wavefield characteristics and shear-velocity profiles from two-dimensional small-aperture arrays analysis of ambient vibrations in a small-size alluvial basin, Colfiorito, Italy*, Bull. Seism. Soc. Am., *96*, 1915–1933.

DI GIULIO, G., IMPROTA, L., CALDERONI, G., and ROVELLI, A. (2008), *A study of the seismic response of the city of Benevento (southern Italy) through a combined analysis of seismological and geological data*, Engin. Geol., *97*, 146–170.

DI NOCERA, S., MATANO, F., PESCATORE, T., PINTO, F., QUARANTIELLO, R., SENATORE, M.R., and TORRE, M. (2006), *Schema geologico del transetto Monti Picentini orientali—Monti della Daunia meridionali: unità stratigrafiche ed evoluzione tettonica del settore esterno dell'Appennino meridionale*, Boll. Soc. Geol. It., *125*, 39–58.

FÄH, D., KIND, F., and GIARDINI, D. (2001), *A theoretical investigation of average H/V ratios*. Geophys, J. Int., *145*, 535–549.

FÄH D., KIND F., and GIARDINI D. (2003), *Inversion of local S-wave velocity structures from average H/V ratios, and their use for the estimation of site-effects*, Journ. Seismol. *7*, 449–467.

GIULIVO, I., and SANTO, A. (1997), Stratigrafia del sottosuolo e problemi geomorfologico-applicativi della città di Avellino, "Geologia delle grandi aree urbane"—Progetto strategico CNR.

HERAK, M. (2008), *ModelHVSR—a Matlab tool to model horizontal-to-vertical spectral ratio of ambient noise*, Computers Geosci., *34*, 1514–1526.

HORIKE, M., ZHAO, B., and KAWASE, H. (2001), *Comparison of site response characteristics inferred from microtremors and earthquake shear waves*, Bull. Seism. Soc. Am., *91*, 1526–1536.

IBS-VON SEHT, M., and WOLHENBERG, J. (1999), *Microtremor measurements used to map thickness of soft sediments*, Bull. Seism. Soc. Am., *89*, 250–259.

KÖHLER A., OHRNBERGER M., SCHERBAUM F., STANGE S., and KIND F. (2004), *Ambient vibration measurements in the southern Rhine Graben close to Basle*, Ann. Geophys., *47*, 1771–1781.

KÖHLER, A., OHRNBERGER, M., and SCHERBAUM, F. (2006). The relative fraction of Rayleigh and Love waves in ambient vibration wave fields at different European sites, in 3rd Int. Symposium on the Effects of Surface Geology on Seismic Motion, Grenoble, France, Abstract 83.

Konno, K., and Ohmachi, T. (1998), *Ground-motion characteristics estimated from spectral ratio between horizontal and vertical components of microtremors*, Bull. Seism. Soc. Am., *88*, 228–241.

Kramer, S.L. (1996), Geotechnical Earthquake Engineering (Prentice Hall, 1996).

Lachet, C., Hatzfeld, D., Bard, P.Y., Theodulidis, N., Papaioannou, C., and Savvaidis, A. (1996), *Site effects and microzonation in the city of Thessaloniki (Greece). Comparison of different approaches*, Bull. Seism. Soc. Am., *86*, 1692–1703.

Luzi, L., Puglia, R., Pacor, F., Gallipoli, M. R., Bindi, D., and Mucciarelli, M. (2011), *Proposal for a soil classification based on parameters alternative or complementary to Vs,30*. Bull Earthquake Eng., doi:10.1007/s10518-011-9274-2.

Malischewsky P.G., and Scherbaum F. (2004), *Love's formula and H/V-ratio (ellipticity) of Rayleigh waves*, Wave Motion, *40*, 57–67.

Maresca R., Galluzzo D., and Del Pezzo, E. (2006), *H/V spectral ratios and array techniques applied to ambient noise recorded in the Colfiorito Basin, central Italy*, Bull. Seism. Soc. Am., *96*, 490–505.

Meletti, C., and Montaldo, V. (2007), Stime di pericolosità sismica per diverse probabilità di superamento in 50 anni: valori di ag. Progetto DPC-INGV S1 (2006), Deliverable D2, http://esse1.mi.ingv.it/d2.html.

Mucciarelli, M., and Gallipoli, M.R. (2006), Comparison between Vs30 and other estimates of site amplification in Italy, Conference on Earthquake Engineering and Seismology, Geneva, 3–8 Sept., no. 270.

Nakamura, Y. (1989), *A method for dynamic characteristics estimation of subsurface using microtremor on the ground surface*, Q. Rept. Railway Tech. Res. Inst., *30*, 25–33.

Nogoshi, M.,and Igarashi, T. (1970), *On the amplitude characteristics of microtremors (Part 1)*, J. Seism. Soc. Japan, *23*, 264–280.

Nogoshi, M., and Igarashi, T. (1971), *On the amplitude characteristics of microtremor (Part 2)*, J. Seism. Soc. Japan, *24*, 26–40.

Parolai, S., Bormann, P., and Milkreit, C. (2002), *New relationships between Vs, thickness of sediments, and resonance frequency calculated by the H/V ratio seismic noise for the Cologne area (Germany)*, Bull. Seism. Soc. Am., *92*, 2521–2527.

Pilz, M., Parolai, S., Leyton, F., Campos, J., and Zschau, J. (2009), *A comparison of site response techniques using earthquake data and ambient seismic noise analysis in the large urban areas of Santiago de Chile*, Geophys. J. Int., *178*, 713–728.

Pilz, M., Parolai, S., Picozzi,M., Wang, R., Leyton, F., Campos, J., and Zschau, J. (2010), *Shear wave velocity model of the Santiago de Chile basin derived from ambient noise measurements: a comparison of proxies for seismic site conditions and amplification*, Geophys. J. Int., *182*, 355–367.

Rodriguez, V.H.S., and Midorikawa, S. (2002), *Applicability of the H/V spectral ratio of microtremors in assessing site effects on seismic motion*, Earthq. Eng. Struct. Dynamics, *31*, 261–279.

Scherbaum F, Hinzen, K.G, and Ohrnberger, M. (2003), *Determination of shallow shear wave velocity profiles in the Cologne/Germany area using ambient vibrations*, Geophys. J. Int. *152*, 597–612.

SESAME (2004), Guidelines for the Implementation of the *H/V* Spectral Ratio Technique on Ambient Vibrations. Measurements, Processing and Interpretation. SESAME European Research Project WP12—D23.12. http://sesame-fp5.obs.ujf-grenoble.fr/Papers/HV_User_Guidelines.pdf.

Souriau, A., Roullé, A., and Ponsolles, C. (2007), *Site effects in the city of Lourdes, France, from H/V measurements: implications for seismic-risk evaluation*, Bull. Seism. Soc. Am., *97*, 2118–2136.

Tokimatsu, K., and Miyadera, Y. (1992), *Characteristics of Rayleigh waves in microtremors and their relation to underground structures*, J. Struct. Constr. Eng. AIJ *439*, 81–87 (in Japanese, English abstract).

Wathelet, M., Jongmans, D., Ohrnberger, M., and Bonnefoy-Claudet, S. (2008), *Array performances for ambient vibrations on a shallow structure and consequences over Vs inversion*, J. Seismol., *12*, 1–19.

Weber, E., Convertito, V., Iannaccone, G., Zollo, A., Bobbio, A., Cantore, L., Corciulo, M., Di Crosta, M., Elia, L., Martino, C., Romeo, A., and Satriano, C. (2007), *An advanced seismic network in the southern Apennines (Italy) for seismicity investigations and experimentation with earthquake early warning*, Seism. Res. Lett., *78*, 622–634.

Wills, C.J., Petersen, M., Bryant, W.A., Reiche, M., Saucedo, G.J., Tan, S., Taylor, G., and Treiman, J. (2000), *A site-conditions map for California based in geology and shear-wave velocity*, Bull. Seism. Soc. Am., *90*, S187–S208.